Modulation of Nuclear Receptor Interactions by Ligands: Kinetic Analysis Using Surface Plasmon Resonance†

Boris Cheskis‡ and Leonard P. Freedman*

Cell Biology & Genetics Program, Memorial Sloan-Kettering Cancer Center, 1275 York Avenue, New York, New York 10021

Received September 25, 1995; Revised Manuscript Received December 19, 1995⊗

ABSTRACT: Many nuclear hormone receptors, including the human 1,25-dihydroxyvitamin D_3 receptor (VDR), bind cooperatively to DNA as either homodimers or heterodimers with the 9-*cis*-retinoic acid receptor (RXR). Protein−protein interactions mediated by residues within both the DNA- and ligand-binding domains contribute to this binding. We have previously reported that the ligands for VDR and RXR can modulate the affinity of the receptors' interaction with DNA [Cheskis, B., & Freedman, L. P. (1994) *Mol. Cell. Biol. 14*, 3329−3338]. To examine this in more detail, we report here the use of surface plasmon resonance (SPR) to characterize the kinetics of both protein−protein and protein−DNA interactions by VDR and RXR in the presence and absence of their cognate ligands. We find that 1,25 dihydroxyvitamin D_3 binding favors both VDR−RXR heterodimerization and, as a result, DNA binding by the complex. Conversely, the ligand reduces VDR homodimerization in solution and the affinity of VDR−DNA interaction. 9-*cis*-Retinoic acid attenuates the stimulating effect of 1,25-dihydroxyvitamin D_3 by decreasing the rate of VDR−RXR heterodimer formation and simultaneously by increasing the affinity of RXR homodimerization. Thus, using SPR, we have shown that a major role for such ligands is to regulate nuclear receptor dimerization both in solution and on DNA. The ligands appear to do so dynamically, modulating the overall affinity of these complexes. This mechanism therefore creates a fast and sensitive way to regulate DNA binding in response to changes in ligand concentration.

Hormonal derivatives of vitamins D and A elicit their signals through nuclear receptors. Though distinct proteins, these receptors are members of a large superfamily related to the steroid hormone receptors and share many common structural and functional features (Amero *et al.*, 1992; Laudet *et al.*, 1992). The retinoid X receptor (RXR) and its cognate ligand (9-*cis*-retinoic acid, 9-*cis*-RA) appear to have a critical role in hormonal signaling, since RXR heterodimerizes with many nuclear receptors, including the vitamin D_3 receptor (VDR), enhancing the binding and transactivation of receptors from appropriate DNA response elements. We and others (Cheskis & Freedman, 1994; Lehmann *et al.*, 1993; Miyamoto *et al.*, 1993; Yen *et al.*, 1992; Zhang *et al.*, 1992) have recently found that a key function of particular ligands is to modulate the receptors' dimerization state. For example, VDR−DNA interaction in the absence of RXR is reduced by 1,25-dihydroxyvitamin D_3 [1,25-$(OH)_2D_3$], but VDR−RXR heterodimer formation on DNA is enhanced by this ligand. 9-*cis*-RA has the opposing effect of decreasing the formation of the heterodimeric complex, while promoting RXR homodimerization on a RXR-specific binding site (i.e., RXRE). These differential effects of ligands on the dimerization state observed *in vitro* could potentially create a sensitive response to fluctuations in intracellular ligand concentrations and the concomitant response by particular target genes to such changes. Here, using surface plasmon resonance (SPR) techniques, we extend these results by demonstrating that ligand modulation of VDR homo- and heterodimerization directly influences the rates of VDR and VDR−RXR association and dissociation at the levels of both protein−protein and protein−DNA interactions.

MATERIALS AND METHODS

Equipment and Reagents. The BIAcore system, sensor chips CM 5 (certified), Tween-20, the amine coupling kit containing *N*-hydroxysuccinimide, *N*-ethyl-*N*′-(3-diethylaminopropyl)carbodiimide (EDC) and ethanolamine hydrochloride, and anti-GST binding kit were all obtained from Pharmacia Biosensor AB. The buffer used for all experiments was 10 mM HEPES, 150 mM NaCl, 3.4 mM EDTA, and 0.05% Tween-20, pH 7.4 (HBS). Crystalline 1,25-$(OH)_2$-D_3 and 9-*cis*-RA were kind gifts of Dr. Milan Uskokovic (Hoffman-La Roche, Nutley, NJ) and Dr. Roger Clerc (Hoffman-La Roche, Basel, Switzerland), respectively.

Biotinylation of Oligonucleotide. A 69 bp oligonucleotide containing a specific binding site for VDR derived from the mouse Spp-1/osteopontin response promoter (Noda *et al.*, 1990) was synthesized as a self-annealing oligonucleotide that forms a hairpin duplex upon heating and quick cooling. Its sequence is 5′-AGCTGAGACGTGAACCTCGTGAACCTTGTTACTCCCCCCGAGCAACAAGGTTCACGAGGTTCACGTCTC-3′. Following annealing, the oligonucleotide was biotinylated by incorporation of biotin-dATP with Klenow enzyme and purified from unincorporated biotinylated nucleotides by gel filtration on a Chromaspin 10 column (Clontech).

† This work was supported by Public Health Service grants DK45460 and CA08748 from the NIH. B.C. was supported by a grant from the New York Community Trust. L.P.F. is a Scholar of the Leukemia Society of America.

* Address correspondence to this author.

‡ Present address: Department of Nuclear Receptors, Wyeth-Ayerst Research, 145 King of Prussia Road, Radnor, PA 19087.

⊗ Abstract published in *Advance ACS Abstracts,* February 15, 1996.

0006-2960/96/0435-3309$12.00/0

Preparation of the Sensor Chip. To immobilize specific DNA, the surface of a CM 5 sensor chip (certified) was modified with streptavidin according to instructions from the manufacturer. Three different surfaces with 145, 450, and 817 resonance units (RU) of DNA were obtained by injecting 20 μL of specific biotinylated oligonucleotide that had concentrations from 20 to 100 μg/mL. After each protein injection, the surface was regenerated with one 10 μL injection of 0.1% SDS solution containing 3.3 mM EDTA. One cycle of regeneration was sufficient to remove bound VDR and/or VDR−RXR.

To immobilize VDR or RXR, anti-glutathione-S-transferase (GST)-antibody was first immobilized on the surface of sensor chip using the amine coupling kit provided with sensor chips by the manufacturer. After injections of 20 μL of purified GST−RXR or GST−VDR (0.2 mg/mL), surfaces with approximately 300 RU of immobilized receptor were obtained. Following each injection, the surface was regenerated with one 5 μL injection of 0.03% SDS solution. To remove immobilized GST−VDR or GST−RXR from the surface of the sensor chip, a 10 μL injection of 10 mM glycine, pH 2.0, was used.

Overexpression and Purification of VDR and GST−RXR. VDR was expressed and purified to homogeneity as previously described (Cheskis & Freedman, 1994). GST−VDR and GST−RXR were overexpressed in *Escherichia coli* (Freedman *et al.*, 1994a) and purified by chromatography on glutathione-agarose and gel-filtration on Superdex-200. HBS buffer was used for the gel-filtration.

Binding Assay and Data Analysis. Each binding cycle was performed with a constant flow of HBS of 5 μL/min. Samples of VDR or GST−RXR or a mix of VDR and GST−RXR were injected across the surface via a sample loop. Once the injection plug had passed the surface, the formed complex was washed with HBS buffer for an additional 500−1000 s to dissociate bound analyte. All experiments were performed at 25 °C. Data were collected at 2 Hz and analyzed using the BIAEvaluation program 2.1 (Pharmacia Biosensor AB) on a Compaq PC. This program uses a nonlinear least-squares analysis method for the determination of rate binding constants for macromolecular interactions.

RESULTS

The BIAcore Biosensor system (Pharmacia Biosensor, Uppsala, Sweden) permits the monitoring of macromolecular interactions in real time. The detection system uses surface plasmon resonance (SPR), a quantum mechanical phenomenon which detects changes in the refractive index at the surface of thin gold film on a glass support (i.e., sensor chip) (Karlsson et al., 1991). A hydrogel matrix on the gold surface of these sensor chips allows for the fast and efficient covalent immobilization of ligands. The chip surface carries a carboxymethylated dextran polymer to which one of the reactants is covalently linked, while the other is introduced in flow over the surface. When a soluble ligand binds to the immobilized one, it leads to an increase in the ligand concentration at the sensor surface, with a corresponding increase in the refractive index. This refractive index change alters the SPR which can be detected optically (Lofas & Johnson, 1990). Binding is measured in arbitrary response units (RU), and a linear relationship exists between the mass of ligand bound to the dextran matrix and the RU observed.

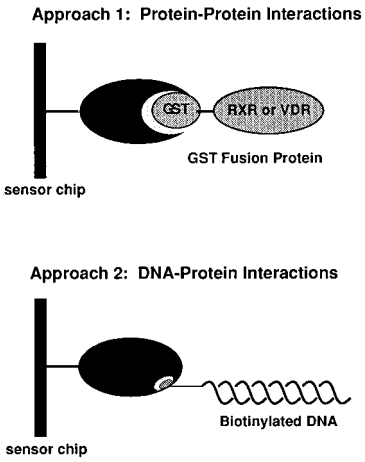

FIGURE 1: Experimental approaches. Two schemes were used to evaluate protein−protein and protein−DNA interactions utilizing the BIAcore. To study VDR homo- or heterodimerization (top), anti-GST-antibody was immobilized on the surface of a sensor chip by standard Pharmacia Biosensor protocol. A surface with approximately 300 RU of immobilized GST−RXR or GST−VDR was obtained by injections of 20 μL of these proteins at a concentration of 0.2 mg/mL, as described in Materials and Methods. To study receptor−DNA interactions (bottom), streptavidin at concentration 50 μg/mL was immobilized by an amine coupling protocol, described by Pharmacia Biosensor. The surface with specific DNA immobilized was then obtained after injection of 20 μL of a 69 bp biotinylated oligonucleotide, synthesized as a self-annealing hairpin duplex.

A signal of 1000 RU corresponds to a surface concentration change of approximately 1 ng/mm^2 (Graznow & Reed, 1992).

We approached our study of how specific ligands affect VDR homo- and heterodimerization using SPR by examining both protein−protein and protein−DNA interactions. We found that direct immobilization of VDR on the surface of the sensor chip by hydroxysuccinimide/carbodiimide method completely abolished its interaction with specific DNA and with RXR (data not shown). Among the possible reasons for this is that amino acids which participate in this interaction were modified in some nonfunctional manner and/or that some sort of sterical hindrance interfered with dimerization. To circumvent this, we have used two approaches, as outlined in Figure 1. To examine receptor−DNA interactions, streptavidin was first covalently immobilized on the surface of the sensor chip, and biotinylated DNA was then attached by streptavidin−biotin interaction. To examine homo- or heterodimerization in the absence of DNA, covalent immobilization of anti-glutathione-S-transferase (GST) antibodies followed by the capturing of GST−VDR or GST−RXR fusion proteins through antibody−antigen interactions was carried out.

Effect of 1,25-Dihydroxyvitamin D_3 on VDR−RXR Heterodimerization. RXR is the heterodimeric partner of VDR. In our previous work, we demonstrated that while 1,25-$(OH)_2D_3$ decreased the affinity of VDR homodimers on specific DNA, the ligand enhanced formation of DNA-bound VDR−RXR heterodimers (Cheskis & Freedman, 1994). At the time, it was not clear whether or not VDR−RXR heterodimer formation was directly promoted by 1,25-$(OH)_2D_3$ and whether or not dimers could form in solution. In order to address these questions, we examined the effect of ligand on heterodimerization by determining affinity of VDR−RXR interaction in the absence of DNA.

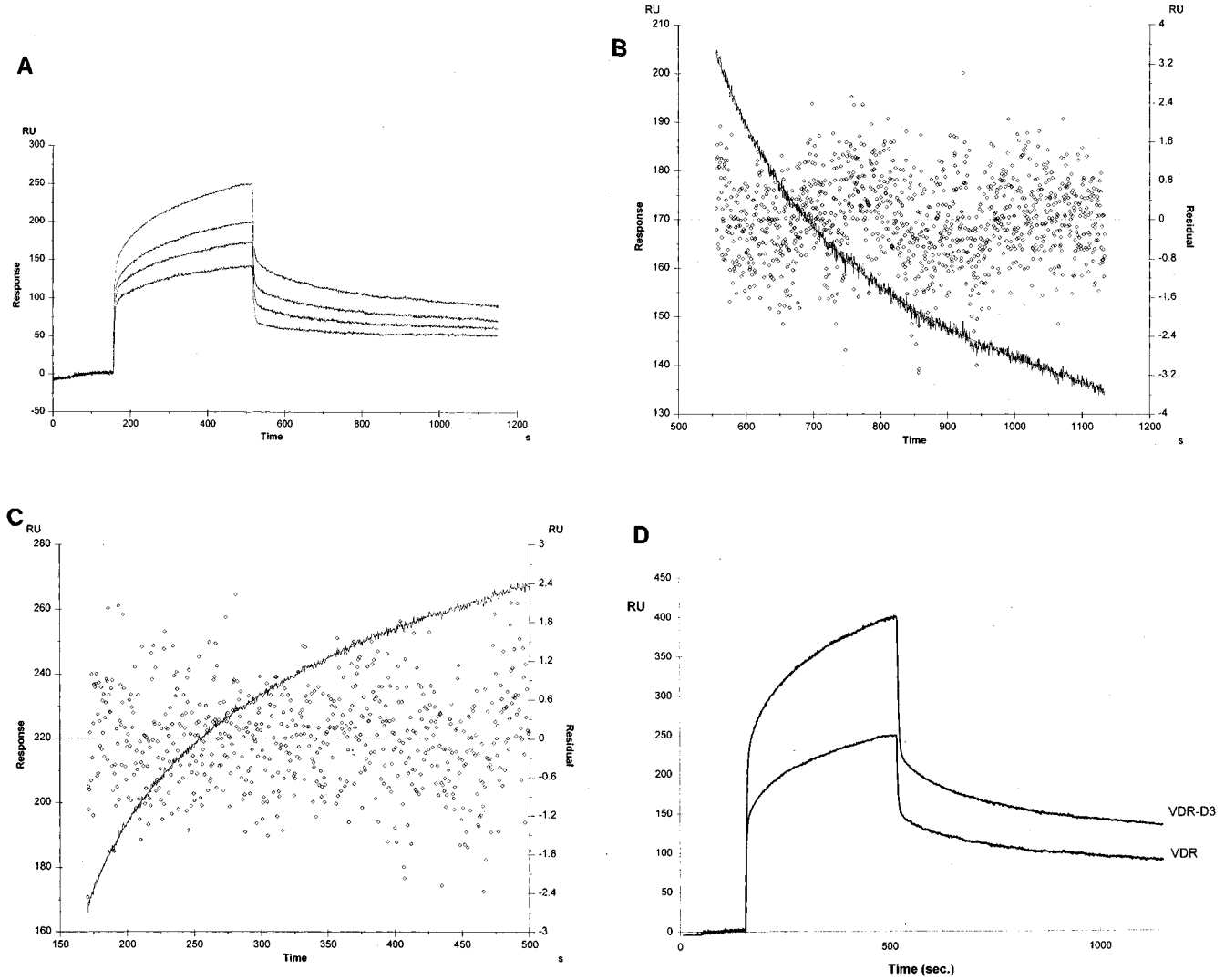

FIGURE 2: Effect of 1,25-$(OH)_2D_3$ on VDR−RXR heterodimerization. (A) Overlayed sensograms showing injections of VDR at a concentration of 0.73, 1.46, 2.92, and 7.3 μM with 320 RU of GST-RXR immobilized on the surface of a sensor chip. (B) Analysis of VDR−RXR complex dissociation using $A_jB_j = A_j + B_j$ model (see text) generated with the BIAevaluation 2.1 program (Biosensor-Pharmacia). Experimental and calculated (fitted) data, and residuals, are presented. $\chi^2 = 0.76$. $k_{d1} = 7.42 \times 10^{-2}$ (s^{-1}); standard error, 1.34×10^{-4}. $k_{d2} = 2.60 \times 10^{-4}$ (s^{-1}); standard error, 7.57×10^{-6}. (C) Analysis of VDR−RXR association rate using the $A + B_1 + B_2 = AB_1 + AB_2$ model. Experimental and calculated (fitted) data, and residuals, are presented. $\chi^2 = 0.89$. $k_{a1} = 5.44 \times 10^3$ (M^{-1} s^{-1}); standard error, 1.11×10^3. $k_{a2} = 921$ (M^{-1} s^{-1}); standard error, 129. (D) 1,25-$(OH)_2D_3$ binding enhances the affinity of VDR−RXR interaction. Two overlayed sensograms of injections of 7.3 μM of liganded and unliganded VDR over the surface with GST-RXR immobilized are shown.

Anti-GST antibody was immobilized by a standard amine coupling protocol, using hydroxysuccinimide (see Materials and Methods), and then GST−RXR was immobilized through GST-capture on the anti-GST sensor chip. After injections of 20 μL of GST-RXR at a protein concentration of 0.2 mg/mL, surfaces with approximately 300 RU of immobilized RXR were obtained. Injections of VDR at concentration ranging from 0.13 to 7.3 μM were then run over the surface (Figure 2A). Examination of these experiments shows that there is an "injection jump" at the beginning and end of each injection due to the difference in the refractive index between the running and sample buffers (presumeably due to small changes in salt concentration). However, after approximately 8 s, the system reaches equilibrium, and data generated can be used for calculations of association and dissociation rates. Sensograms were analyzed using the BIAevaluation 2.1 program. This program uses a nonlinear least-squares analysis method for determination of rate constants for macromolecular interaction. The dissociation kinetics of the heterodimeric VDR−RXR complex can be described by a double-exponential decay, defined as

$$R_{(t)} = R_{1(t_o)}e^{-k_{d1}(t-t_o)} + R_{2(t_o)}e^{-k_{d2}(t-t_o)} \quad (1)$$

and

$$R_1 + R_2 = R \text{ (observed)}$$

were t_o defines the starting point for the injection, R_1 is the amplitude of the dissociation with a rate constant $-k_{d1}$, and R_2 is the amplitude of the dissociation with a rate constant $-k_{d2}$. A single-exponential decay results in nonrandom and large residuals, whereas a double-exponential fit results in residuals which are significantly smaller and more random (see Figure 2B). In addition, χ^2 value is significantly smaller for a two-exponential decay.

The apparent dissociation rate constants determined for VDR−RXR interaction in the absence of ligand were: k_{d1}

$= 0.072 \pm 0.012\ s^{-1}$ and $k_{d2} = 2.6 \pm 0.12 \times 10^{-4}\ s^{-1}$. For the liganded VDR, apparent dissociation rate values were similar: $k_{d1} = 0.074 \pm 0.053\ s^{-1}$ and $k_{d2} = 2.3 \pm 0.14 \times 10^{-4}\ s^{-1}$. Fast dissociation in both cases had an amplitude of approximately 10% of the total dissociation process.

Several models were considered to describe association of VDR with immobilized GST−RXR. A monomolecular interaction, where A + B = AB, does not describe it well, resulting in nonrandom and large residuals. A good description for liganded and unliganded VDR association with GST−RXR was obtained using a model where one analyte can interact with two independent binding sites: $A + B_1 + B_2 = AB_1 + AB_2$ (Figure 2C). The association phase is fit according to

$$R_{(t)} = R_{eq1}(1 - e^{-(k_{a1}C_1n_1+k_{d1})(t-t_o)}) + R_{eq2}(1 - e^{-(k_{a2}C_2n_2+k_{d2})(t-t_o)}) \quad (2)$$

where

$$R_{eq1} = k_{a1}C_1R_{max1}/(k_{a1}C_1n_1 + k_{d1})$$

$$R_{eq2} = k_{a2}C_2R_{max2}/(k_{a2}C_2n_2 + k_{d2})$$

$$R_{max1} + R_{max2} = R_{max}\ (\text{observed})$$

where k_{a1} and k_{d1} are the apparent rate constants describing one type of interaction with an equilibrium signal R_{eq1}, and k_{a2} and k_{d2} are the apparent rate constants describing the second type of interaction with an equilibrium signal R_{eq2}; C is the analyte concentration; and n_1 and n_2 are the number of binding sites that are blocked when analyte reacts with the immobilized ligand (i.e, GST−RXR). k_{d1} and k_{d2} were used as fixed parameters during the fitting procedure. As can be seen in Figure 2C, the residuals are small and random. Using this equation, the apparent association rate constants calculated from the sensograms obtained by the serial injections of VDR are $k_{a1} = 3.12 \pm 0.28 \times 10^3\ M^{-1}\ s^{-1}$ and $k_{a2} = 920 \pm 120\ M^{-1}\ s^{-1}$, and $k_{a1} = 7.87 \pm 0.49 \times 10^3\ M^{-1}\ s^{-1}$ and $k_{a2} = 5.7 \pm 0.348 \times 10^3\ M^{-1}\ s^{-1}$ for VDR-D_3. Analysis of VDR interaction with immobilized GST−RXR therefore suggests that there are at least two types of complexes that can be formed. Since the control experiment, injection of VDR over the surface with anti-GST-antibody immobilized, does not show any significant interaction (data not shown), it is possible that the first complex (approximately 10% of bound material), where the association rate is fast and its stability is low, may be due to heterogeneity of the immobilized GST−RXR. Another possible reason is that formation of a stable VDR−RXR heterodimeric complex undergoes several states, some of which are unstable.

The apparent equilibrium dissociation constants for the second complex, which represent the majority of bound material, were calculated from the two rate constants ($K_D = k_{d2}/k_{a2}$); for unliganded VDR, $K_D = 2.82 \times 10^{-7}$ M, for VDR-D_3, $K_D = 4.0 \times 10^{-8}$ M. Thus, the two receptors interact strongly in the absence of DNA, and it is apparent from the data that liganded VDR has a much higher affinity for RXR than does unliganded VDR. Figure 2D presents two overlayed sensograms obtained by injections of liganded and unliganded VDR (at the same protein concentration) over the surface with GST-RXR immobilized. The sensograms clearly show that ligand binding significantly enhances the affinity of VDR−RXR interaction in the absence of DNA, doing so by affecting primarily the association rates.

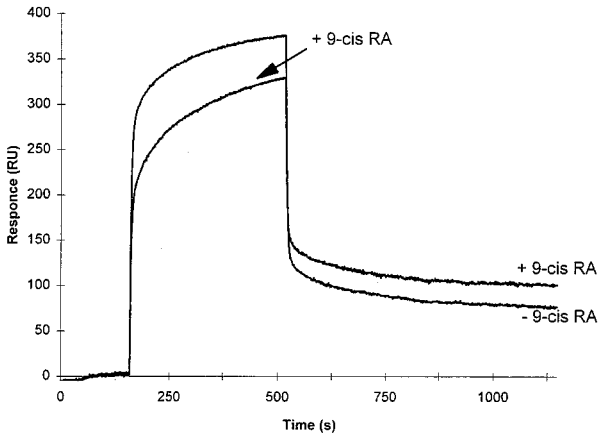

FIGURE 3: 9-*cis*-RA binding enhances the affinity of RXR homodimerization. Two overlayed sensograms depicting injections of 1.45 μM of liganded and unliganded GST-RXR over the surface with GST-RXR immobilized are shown.

Effect of 9-cis-Retinoic Acid on RXR−RXR Homodimerization. It has been shown that 9-*cis*-RA enhances RXR homodimerization on a RXR-specific binding site (RXRE, a direct repeat hexamer with a spacing of 1 base pair) (Zhang *et al.*, 1992). Since GST−RXR was immobilized on the surface of a sensor chip, we asked if 9-*cis*-RA could affect RXR homodimerization in the absence of DNA. Injections of liganded and unliganded GST−RXR at a concentration range from 0.1 to 7 μM were run over the surface with 300 RU of GST−RXR immobilized. Figure 3 presents two overlayed sensograms obtained by injections of liganded and unliganded GST-RXR (at the same protein concentration) over the surface with GST−RXR immobilized. It is apparent from the sensogram that ligand binding increases the affinity of RXR homodimerization. Similar results were obtained over the entire range of GST−RXR concentrations (data not shown). Unfortunately, it was not possible to determine affinity constants for GST−RXR homodimerization because the control that was used (injections of GST protein over the surface) showed some unspecific interaction (data not shown).

Effect of 1,25-Dihydroxyvitamin D_3 on VDR−VDR Homodimerization. We and others have previously demonstrated that VDR can bind as a homodimer to particular vitamin D response elements (VDRE) (Cheskis & Freedman, 1994; Freedman *et al.*, 1994a; Towers *et al.*, 1993; Nishikawa *et al.*, 1995). Using the protein−protein interaction evaluation approach described above for VDR−RXR and RXR−RXR interactions, we asked if VDR could homodimerize in the absence of DNA, and how 1,25-$(OH)_2D_3$ affected this interaction. GST−VDR was overexpressed in *E. coli* and purified by chromatography on glutathione-agarose (Freedman *et al.*, 1994a) and by gel filtration. A surface with 300 RU of immobilized GST-VDR was obtained by injection of 20 μL of 0.2 mg/mL GST−VDR over a chip surface containing immobilized anti-GST-antibody. Injections of liganded and unliganded VDR at a concentration range from 130 nM to 14.6 μM were run over the surface. The dissociation kinetics of the VDR−VDR complex can be described as a double-exponential decay according to eq 1 (two-component dissociation) with two apparent dissociation

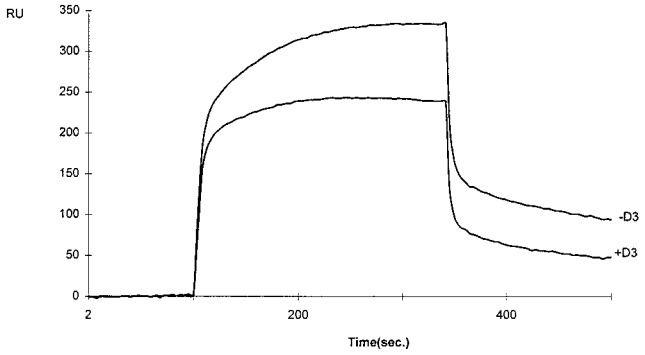

FIGURE 4: 1,25-$(OH)_2D_3$ binding decreases VDR homodimerization in the absence of DNA. Two overlayed sensograms of injections of 2.92 μM of liganded and unliganded VDR over the surface with GST-VDR immobilized are shown.

Table 1: Summary of Rate and Affinity Constants Receptor−Receptor Interactions

k_d (s^{-1})	k_a (M^{-1} s^{-1})	K_D (M)
(1) 350 RU of GST−RXR Immobilized		
(a) GST−RXR + VDR		
$2.60 \pm 0.32 \times 10^{-4}$	920 ± 175	2.82×10^{-7}
(b) GST−RXR + VDR−D_3		
$2.34 \pm 0.47 \times 10^{-4}$	$5.73 \pm 0.3 \times 10^3$	4.08×10^{-8}
(2) 300 RU of GST−VDR Immobilized		
(a) GST−VDR + VDR		
$4.52 \pm 0.37 \times 10^{-4}$	732 ± 89	6.17×10^{-7}
(b) GST-VDR + VDR-D3		
$8.73 \pm 0.48 \times 10^{-4}$	345 ± 41	2.53×10^{-6}

rate constants: $k_{d1} = 0.021 \pm 0.012$ s^{-1} and $k_{d2} = 4.52 \pm 0.12 \times 10^{-4}$ s^{-1}. For the liganded VDR, apparent dissociation rate values are $k_{d1} = 0.01 \pm 0.0053$ s^{-1} and $k_{d2} = 8.73 \pm 0.10 \times 10^{-4}$ s^{-1}. Fast dissociation in both cases had an amplitude of approximately 10% of the total dissociation process.

A good description for liganded and unliganded VDR association with immobilized GST−VDR was obtained using a model which describes one analyte interaction with two independent binding sites: $A + B_1 + B_2 = AB_1 + AB_2$. As was the case with the VDR−RXR heterodimer, a monomolecular interaction, where $A + B = AB$, does not describe the interaction satisfactorily, resulting in nonrandom and large residuals. The apparent association rate constants calculated from the eq 2 were $k_{a1} = 5.86 \pm 0.43 \times 10^3$ M^{-1} s^{-1} and $k_{a2} = 732 \pm 89$ M^{-1} s^{-1} for unliganded VDR and $k_{a1} = 6.14 \pm 0.37 \times 10^3$ M^{-1} s^{-1} and $k_{a2} = 345 \pm 41$ M^{-1} s^{-1} for VDR-D_3. The apparent equilibrium dissociation constants were calculated as $K_D = k_{d2}/k_{a2}$, for unliganded VDR, $K_D = 6.17 \times 10^{-7}$ M, for VDR-D_3, $K_D = 2.53 \times 10^{-6}$ M. Figure 4 presents two overlayed sensograms obtained by injections of liganded and unliganded VDR (at the same protein concentration) over the surface with GST−VDR immobilized, demonstrating that ligand binding significantly decreases the affinity of VDR−VDR interaction in the absence of DNA, by affecting both association and dissociation rates. Table 1 summarizes these results.

VDR Interaction with Specific DNA. To examine the kinetics of VDR binding to specific DNA elements, three surfaces with different levels of DNA density (145, 450, and 817 RU) were prepared (see Material and Methods) using an oligonucleotide duplex containing a specific VDRE derived from the mouse osteopontin (Spp-1) gene promoter (Noda *et al.*, 1990). As mentioned above, we have previously shown that this VDRE is a relatively strong binding site for both VDR homodimers and VDR−RXR heterodimers in vitro (Cheskis & Freedman, 1994; Freedman *et al.*, 1994a).

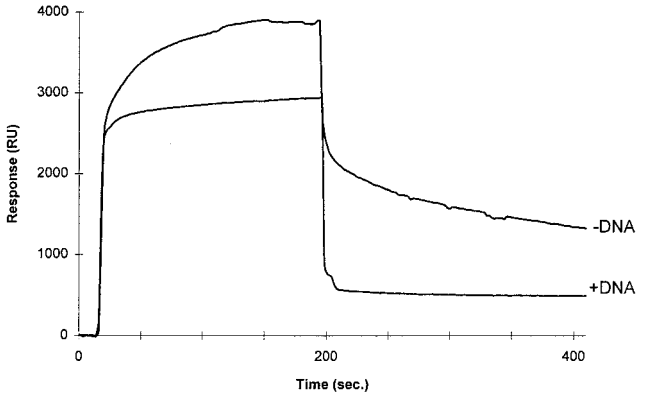

FIGURE 5: VDR−RXR binding to specific DNA can be almost completely abolished by addition of specific competitor DNA. Two overlayed sensograms of 0.7 μM of VDR and GST-RXR injected over the surface with 817 RU of a DNA oligonucleotide duplex containing a VDRE immobilized on a surface of sensor chip.

The amount of DNA immobilized on the surface of a sensor chip is crucial for the evaluation of protein−DNA interactions. We found that a low density surface (145 RU of immobilized specific DNA) gives a low signal-to-noise ratio with VDR injected over the surface but yields a reasonable signal with a VDR−RXR mix injected (since the heterodimeric complex interacts with DNA with a higher affinity than does the homodimer; see below). To study the effect of ligands on both homo- and heterodimeric formation on DNA, we used 817 RU surface of immobilized DNA, which gives a satisfactory level of signal in both cases.

The sensogram depicted in Figure 5 demonstrates that VDR−RXR binding to the immobilized DNA can be almost completely abolished by addition of an excess of unbound specific competitor DNA. Thus, the mass increase on the surface of the sensor chip in response to the injection of VDR−RXR is due to specific binding to DNA. Injections of VDR or VDR−RXR over the surface with no DNA immobilized gave no detectable binding (data not shown).

An example of an analysis of the kinetics of VDR−DNA interactions with specific DNA is presented in Figure 6. To obtain association and dissociation rates of VDR−DNA complexes in the absence of RXR, serial injections of unliganded VDR at concentrations ranging from 73 nM to 2.3 μM were run over the surface of a VDRE-immobilized sensor chip (Figure 6A). As before, sensograms were analyzed using BIAevaluation program 2.1.

The dissociation phase data cannot be described well as a single-exponential decay but rather can more accurately be described by a double-exponential decay (Figure 6B) according to eq 1. A single-exponential fit results in nonrandom and large residuals, whereas a double-exponential fit results in residuals which are significantly smaller and more random. Moreover, the χ^2 value is significantly smaller for a two-exponential decay model. A comparison of single- and double-exponential fits suggest that there are at least two types of complexes that VDR can form with DNA immobilized on the surface of a sensor chip. The apparent

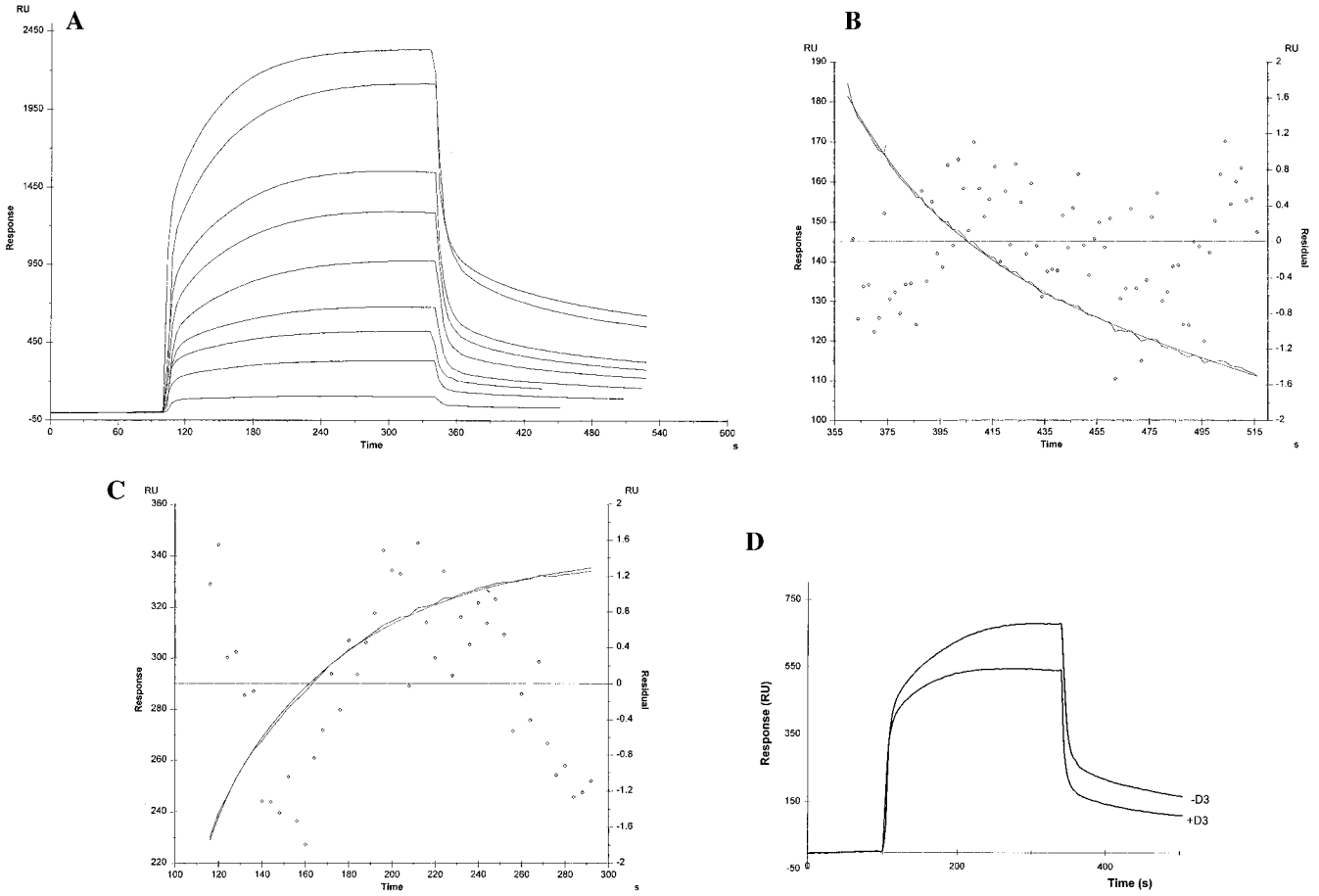

FIGURE 6: Kinetics of VDR−DNA binding in the absence of RXR. (A, top left) Serial injections of VDR at concentrations 0.07, 0.22, 0.37, 0.51, 0.62, 0.87, 1.17, 1.60, and 2.30 μM over the surface with 817 RU of specific DNA immobilized. (B, top right) Analysis of VDR-DNA dissociation rate ($A_jB_j = A_j + B_j$ model). Experimental and calculated (fitted) data, and residuals, are presented. $\chi^2 = 0.78$. $k_{d1} = 0.05$ (s^{-1}); standard error, 6.35×10^{-3}. $k_{d2} = 2.72 \times 10^{-3}$ (s^{-1}); standard error, 1.25×10^{-4}. (C, bottom left) Analysis of VDR-DNA association rate using the $A_1 + A_2 + B = A_1B + A_2B$ model. Experimental and calculated (fitted) data, and residuals, are presented. $\chi^2 = 0.91$. $k_{a1} = 1.86 \times 10^5$ (M^{-1} s^{-1}); standard error, 1.07×10^4. $k_{a2} = 2.53 \times 10^4$ (M^{-1} s^{-1}); standard error, 1.09×10^3. (D) 1,25-$(OH)_2D_3$ binding by VDR significantly inhibits the formation of a VDR−DNA complex. Two overlayed injections of 0.51 μM of liganded and unliganded VDR over the surface with specific DNA immobilized are presented.

dissociation rate constants determined for these data were $k_{d1} = 0.093 \pm 0.025$ s^{-1} and $k_{d2} = 2.5 \pm 0.43 \times 10^{-3}$ s^{-1}.

Since VDR binds the osteopontin VDRE as a homodimer and as a low cooperativity monomer (Cheskis & Freedman, 1994), we have assumed that the two rates reflect monomer and dimer dissociation from DNA. Note that in our previous experiments (see above), where we examined the ability of VDR to homodimerize in the absence of DNA, we also observed that two molecular forms of VDR exist in solution, presumably a monomer and homodimer, which we assume can both bind DNA. To find the association rates for VDR binding to DNA, we have therefore used a model which describes two analytes (A_1 and A_2) interacting with the same binding site: $A_1 + A_2 + B = A_1B + A_2B$ (Figure 6C). The association phase is fit according to

$$R_{A1}(t) = \frac{R_{max} k_{a1} C_1}{K_f - K_s} \times \left(\frac{k_{d2}(K_f - K_s)}{K_f K_s} + \frac{k_{d2} - K_f}{K_f} e^{-K_f(t-t_o)} - \frac{k_{d2} - K_s}{K_s} e^{-K_s(t-t_o)} \right) \quad (3)$$

and

$$R_{A2}(t) = \frac{R_{max} MW_2 k_{a2} C_2}{(K_f - K_s) MW_1} \times \left(\frac{k_{d1}(K_f - K_s)}{K_f K_s} + \frac{k_{d1} - k_f}{K_f} e^{-K_f(t-t_o)} - \frac{k_{d1} - K_s}{K_s} e^{-K_s(t-t_o)} \right)$$

where

$$K_f = 0.5(K_A + K_B + ((K_A - K_B)^2 + 4k_{a1}k_{a2}C_1C_2)^{0.5})$$

$$K_s = 0.5(K_A + K_B - ((K_A - K_B)^2 + 4k_{a1}k_{a2}C_1C_2)^{0.5})$$

$$K_A = k_{a1}C_1 + k_{d1}$$

$$K_B = k_{a1}C_2 + k_{d2}$$

k_{a1} and k_{a2} are the apparent association rate constants, and k_{d1} and k_{d2} are the dissociation rate constants for a monomer and dimer, respectively. These constants were used as fixed parameters during the fitting procedure. C_1 and C_2 are the

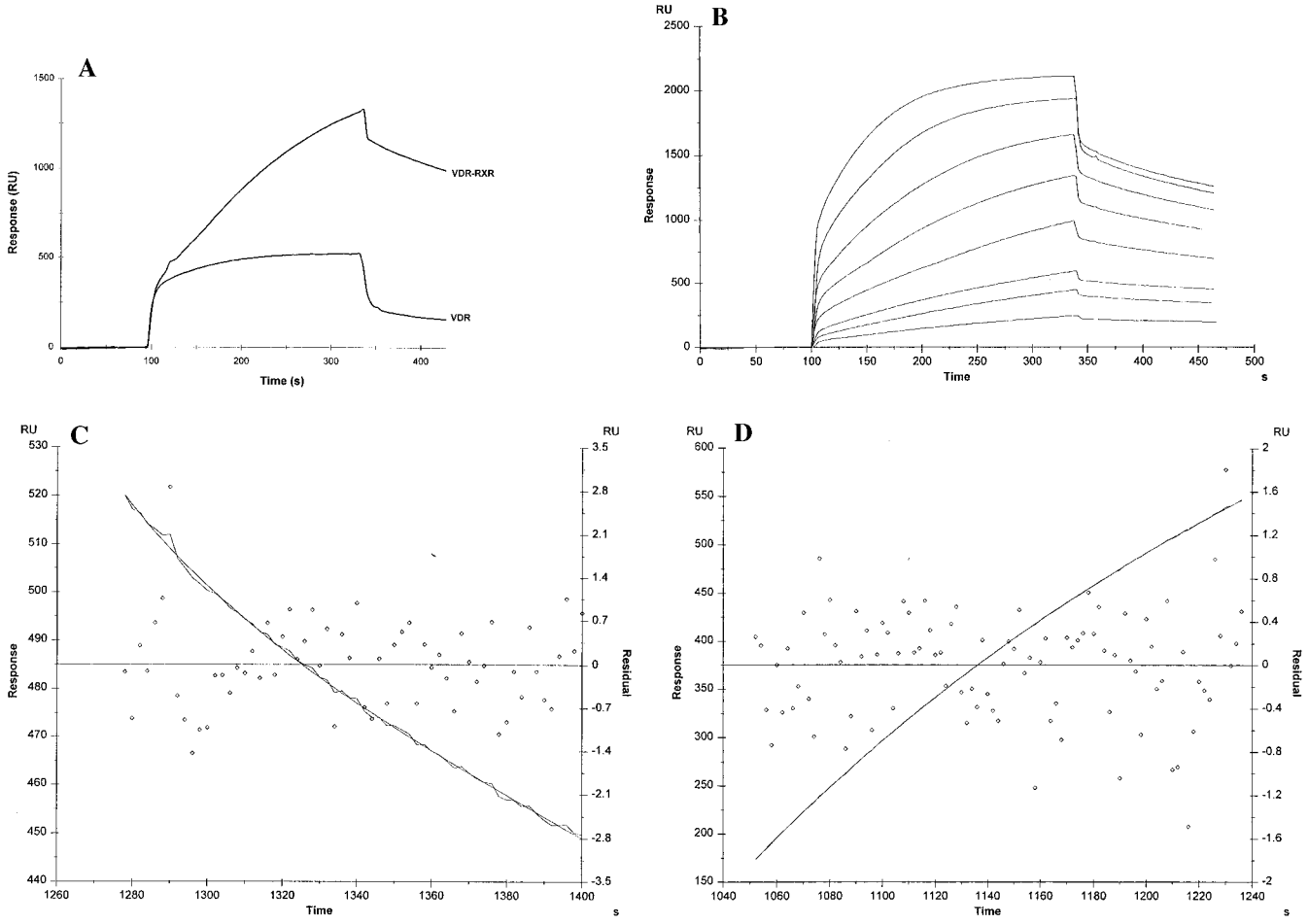

FIGURE 7: VDR−RXR binding to DNA. (A) VDR−RXR complex binds DNA with much higher affinity than VDR alone. Two overlayed sensograms of injections of 0.51 μM of VDR and mix of VDR at the same concentration and GST-RXR at concentration 1.53 μM over the surface with Spp-1 VDRE DNA immobilized. (B, top right) Dose−response of VDR−RXR injections**.** Serial injections of VDR at concentrations 0.013, 0.073, 0.145, 0.291, 0.51, 0.75, 1.15, and 2.3 μM mixed with GST-RXR at molar ratio 1:3 over the surface with 817 RU of Spp-1 VDRE DNA immobilized are shown. (C, bottom left) Analysis of VDR−RXR dissociation from DNA ($A_jB_j = A_j + B_j$ model). Experimental and calculated (fitted) data, and residuals, are presented. $\chi^2 = 0.53$. $k_{d1} = 0.032$ (s^{-1}); standard error, 1.19×10^{-3}. $k_{d2} = 1.20 \times 10^{-3}$ (s^{-1}); standard error, 2.13×10^{-4}. (D, bottom right) Analysis of VDR−RXR−DNA association rate using the $A_1 + A_2 + B = A_1B + A_2B$ model. Experimental and calculated (fitted) data, and residuals, are presented. $\chi^2 = 0.91$. $k_{a1} = 1.86 \times 10^5$ (M^{-1} s^{-1}); standard error, 1.07×10^4. $k_{a2} = 7.14 \times 10^4$ (M^{-1} s^{-1}); standard error, 1.09×10^3.

concentrations (M) of monomer and homodimer in solution which were calculated based on the Law of Mass Action:

$$2\mathrm{VDR} \rightarrow \mathrm{VDR}_2$$

and

$$[\mathrm{VDR}]^2/[\mathrm{VDR{-}VDR}] = K_D \qquad (4)$$

K_D for VDR homodimerization was found by injections of VDR over the surface with immobilized GST-VDR (see above). MW_1 and MW_2 are the molecular weights (Da) of the monomer and homodimer, R_{max} is the maximum capacity for VDR on a surface (RU), and t_o is a start of injection. As can be seen in Figure 6C, the residuals are small and random. Using this equation, the apparent association rate constants calculated from the sensograms obtained by the serial injections of VDR are $k_{a1} = 1.95 \pm 0.27 \times 10^5$ M^{-1} s^{-1}, for monomer association, and $k_{a2} = 2.54 \pm 0.13 \times 10^4$ M^{-1} s^{-1} for the dimer. For the VDR monomer, the apparent equilibrium dissociation constant, calculated as $K_D = k_d/k_a$, is equal to 3.59×10^{-7} M, and for the dimer, $K_D = 9.86 \times 10^{-8}$ M.

Effect of 1,25-Dihydroxyvitamin D_3 on VDR Binding to DNA. To examine the effect of the ligand on VDR binding to DNA, purified VDR was incubated overnight with 100 nM 1,25-$(OH)_2D_3$, and serial injections of 20 μL of protein with a concentration range from 73 nM to 2.3 μM were run over the sensor chip carrying specific DNA immobilized.

Figure 6D presents two overlayed sensograms of liganded and unliganded VDR, injected over a surface with VDRE DNA immobilized. Relative to unliganded VDR, much less protein−DNA complex is formed when VDR is preincubated with 1,25-$(OH)_2D_3$. Analysis of the dissociation phase according to eq 1 (two-component dissociation) gives two apparent dissociation rate constants for VDR-D_3: $k_{d1} = 0.07 \pm 0.020$ s^{-1} and $k_{d2} = 3.5 \pm 0.157 \times 10^{-3}$ s^{-1}. Analysis of the association phase was done assuming possible monomer and dimer interactions with specific DNA according to eq 3. From sensograms generated by the serial injections of VDR-D_3, the association rate constants are: $k_{a1} = 1.53 \pm 0.33 \times 10^5$ M^{-1} s^{-1} for monomer association, and $k_{a2} = 2.03 \pm 0.37 \times 10^4$ M^{-1} s^{-1} for the dimer. For monomeric VDR-D_3, the apparent equilibrium dissociation constant, calculated as $K_D = k_d/k_a$, is equal to 4.26×10^{-7} M, and for dimeric VDR-D_3, the $K_D = 1.72 \times 10^{-7}$ M.

Kinetic analyses of VDR interaction with specific DNA indicates that ligand binding reduces the affinity of VDR−DNA interaction, affecting both the association and dissociation rates. The major effect, however, appears to be on the concentration of homodimer in solution, which then significantly reduces formation VDR dimeric complex bound to DNA.

Effect of 1,25-Dihydroxyvitamin D_3 on VDR−RXR Heterodimerization on DNA. To study VDR−RXR heterodimerization on DNA, we first had to ensure that RXR itself does not interact with immobilized DNA containing the osteopontin VDRE. Typically, RXR binds DNA selectively as a homodimer to a direct repeat element spaced by one base pair (Mangelsdorf *et al*., 1991). Serial injections of GST−RXR were run over the surface with immobilized VDRE, and very low interaction was detected (data not shown). Thus, RXR on its own does not bind specifically to the osteopontin VDRE. Figure 7A presents sensograms of two injections of VDR and VDR−RXR mixtures over the DNA surface. The VDR concentration in both experiments was the same; the optimal VDR/RXR ratio was found by injecting samples with the same concentration of VDR and varying concentrations of GST−RXR. This ratio was then used in all subsequent experiments. The significant differences apparent in the two sensograms (Figure 7A) correlates with differences in affinity between homo- and heterodimeric VDR complexes on DNA.

Unliganded VDR or VDR preincubated with 1,25-$(OH)_2D_3$ was mixed with GST−RXR and injected over the surface with specific DNA immobilized (Figure 7B). The dissociation process for heterodimeric VDR−RXR complexes on DNA in both the absence and presence of ligand can be described as double exponential decays, as defined by eq 1 (Figure 7C). The apparent dissociation rate constant determined in the absence of 1,25-$(OH)_2D_3$ were $k_{d1} = 67 \pm 5.45 \times 10^{-3}$ s^{-1} and $k_{d2} = 1.1 \pm 0.235 \times 10^{-3}$ s^{-1}. In the presence of ligand, the rates were $k_{d1} = 64 \pm 4.24 \times 10^{-3}$ s^{-1} and $k_{d2} = 9.4 \pm 0.87 \times 10^{-4}$ s^{-1}. It is interesting to note that, in both cases, the fast dissociation, which we assume corresponds to the dissociation of VDR monomer from DNA, has an amplitude which is significantly smaller than in the case of VDR alone (Figure 6). The reason for this is that much more of the heterodimer can form when VDR is preincubated with RXR than homodimer in the absence of RXR at the same concentration of VDR. Thus, the ratio between VDR monomer and dimer is much smaller when VDR is preincubated with RXR before the injection than in the absence of RXR.

From the results presented earlier (see Figure 2) and from previous studies using coprecipitation techniques, it is apparent that VDR and RXR can heterodimerize in solution and then, we assume, can interact as a complex with DNA. Given that the concentration of homodimeric VDR is low, and the predominant molecular form of VDR in the presence of RXR is a heterodimer, formation of which is enhanced by 1,25-$(OH)_2D_3$, we have used a model to describe the association process which considers VDR monomeric, and VDR-RXR heterodimeric interaction with specific DNA, described as $A_1 + A_2 + B = A_1B + A_2B$ (Figure 7D). The association phase is fit according to Eq. 3. Concentrations of monomeric VDR and heterodimeric VDR−RXR in solution were calculated based on the Law of Mass Action:

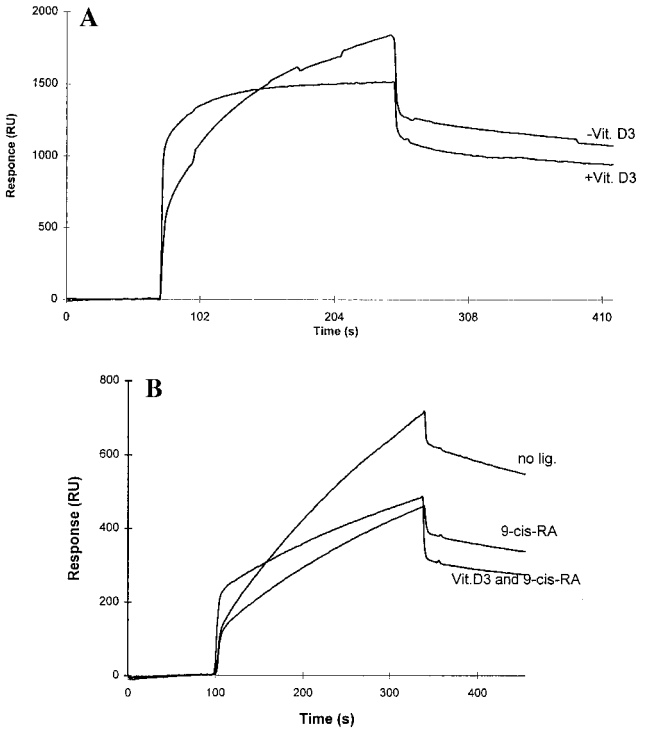

FIGURE 8: Effects of ligands on VDR−RXR interaction with specific DNA. (A, top) Formation of a VDR−RXR heterodimeric complex on DNA is much faster when VDR is liganded. Two overlayed sensograms of liganded and unliganded VDR (1.15 μM) mixed with GST-RXR (3.5 μM), and injected over the surface with Spp-1 VDRE DNA immobilized, are shown. (B, bottom) 9-*cis*-RA binding by GST−RXR significantly reduces affinity of VDR−RXR heterodimerization on DNA. Three overlayed sensograms of mixed unliganded receptors (0.291 μM of VDR and 0.871 μM of GST−RXR), unliganded VDR and liganded GST−RXR, or both liganded receptors, injected over the surface with Spp-1 VDRE DNA immobilized, are shown.

$$\text{VDR} + \text{RXR} \rightarrow \text{VDR}-\text{RXR}$$

and

$$[\text{VDR}][\text{RXR}]/[\text{VDR}-\text{RXR}] = K_D \qquad (4)$$

and used as a fixed parameters. k_{a1} is the apparent association rate constant for the monomer which was determined in previous experiments, and, together with k_{d1} and k_{d2}, the dissociation rate constants for a monomer and heterodimer, respectively, were also used as fixed parameters during the fitting procedure. Figure 7D shows that the model we used describes the experimental data quite well, resulting in random and small residuals. The apparent association rate constant for the heterodimer was calculated from eq 3, $k_{a2} = 7.48 \pm 0.65 \times 10^4$ M^{-1} s^{-1}.

Figure 8A shows two sensograms obtained by injections of liganded and unliganded VDR mixed with GST−RXR over the immobilized VDRE surface. Analysis of the kinetics of VDR-D_3 heterodimerization on the VDRE was done as described above. Values of apparent association and dissociation rates are summarized in Table 2. The results demonstrate that 1,25-$(OH)_2D_3$ binding significantly increases VDR−RXR heterodimerization in solution, which then results in the enhancement of heterodimeric complex formation on DNA.

The Role of 9-cis-Retinoic Acid in VDR−RXR Interaction on DNA. We and others have previously found that 9-*cis*-RA has the opposite effect of 1,25-$(OH)_2D_3$ in that it inhibits

Table 2: Summary of Rate and Affinity Constants Receptor−DNA Interactions

k_d (s^{-1})	k_a (M^{-1} s^{-1})	K_D (M)	
1. VDR + DNA			
$93 \pm 25 \times 10^{-3}$	$1.95 \pm 0.27 \times 10^5$	3.59×10^{-7}	monomer
$2.51 \pm 0.43 \times 10^{-3}$	$2.54 \pm 0.13 \times 10^4$	9.86×10^{-8}	dimer
2. VDR-D3 + DNA			
$71 \pm 4.56 \times 10^{-3}$	$1.53 \pm 0.33 \times 10^5$	4.26×10^{-7}	monomer
$3.54 \pm 0.36 \times 10^{-3}$	$2.03 \pm 0.37 \times 10^4$	1.72×10^{-7}	dimer
3. VDR and RXR + DNA			
$55 \pm 21 \times 10^{-3}$	$1.57 \pm 0.48 \times 10^5$	3.50×10^{-7}	monomer
$1.17 \pm 0.23 \times 10^{-3}$	$7.48 \pm 0.65 \times 10^4$	1.47×10^{-8}	heterodimer
4. VDR-D3 and RXR + DNA			
$64 \pm 14 \times 10^{-3}$	$1.54 \pm 0.78 \times 10^5$	4.15×10^{-7}	monomer
$9.44 \pm 0.93 \times 10^{-4}$	$8.39 \pm 0.67 \times 10^4$	1.08×10^{-8}	heterodimer
5. VDR and RXR−9-*cis*-RA + DNA			
$51 \pm 13 \times 10^{-3}$	$1.75 \pm 0.095 \times 10^5$	2.91×10^{-7}	monomer
$1.14 \pm 0.38 \times 10^{-3}$	$4.32 \pm 0.37 \times 10^4$	2.56×10^{-8}	heterodimer
6. VDR-D3 and RXR−9-*cis*-RA + DNA			
$59 \pm 25 \times 10^{-3}$	$1.75 \pm 0.13 \times 10^5$	3.37×10^{-7}	monomer
$1.37 \pm 0.33 \times 10^{-3}$	$2.24 \pm 0.53 \times 10^4$	5.88×10^{-8}	heterodimer

VDR−RXR binding to a VDRE (Cheskis & Freedman, 1994; MacDonald *et al*., 1993); similar results have been reported for thyroid hormone receptor (Lehman *et al*., 1993). Moreover, 9-*cis*-RA enhances the binding of RXR homodimers to a DR+1 element (Lehmann *et al*., 1993; Zhang *et al*., 1992). In our previous experiments, we have shown that 9-*cis*-RA significantly increases RXR homodimerization (Figure 3A). Thus, we asked how 9-*cis*-RA affects the kinetics of VDR−RXR heterodimerization on a VDRE. GST−RXR was preincubated with 9-*cis*-RA overnight, mixed with VDR-D_3 or unliganded VDR, and used for serial injections over the surface of a sensor chip carrying immobilized VDRE−DNA. Analysis of the affect of 9-*cis*-RA on the kinetics of VDR−RXR interaction with the VDRE was examined as already described. Values of apparent association and dissociation rates are summarized in Table 2. Figure 8B shows that much less of the heterodimer on DNA can be formed in the presence of 9-*cis*-RA−RXR. This ligand-dependent reduction appears to occur because of at least two possibilities: (1) the concentration of monomeric RXR is lower (since RXR homodimerization is enhanced), which in turn may indirectly decrease the concentration of VDR−RXR heterodimers in solution; and (2) the apparent association rate for heterodimeric binding to the VDRE is decreased relative to heterodimer binding in the absence of 9-*cis*-RA. Moreover, when both receptors are liganded, the affinity of the heterodimer−DNA complex is even lower than when only RXR is liganded (Figure 8B). Table 2 summarizes the effects both ligands on VDR and VDR−RXR interaction with specific DNA.

DISCUSSION

In a series of previous studies (Fisher *et al*., 1994a,b; Bondeson *et al*., 1993), surface plasmon resonance-based methodology, such as the BIAcore biosensor, has been effectively used to study in detail protein−DNA interactions. We believe that the work presented here is the first example of how the BIAcore can be utilized to examine how signal transducing, lipophilic ligands, such as 1,25-dihydroxyvitamin D_3 and 9-*cis*-retinoic acid, can modulate protein−protein and protein−DNA interactions that occur between the receptors for these ligands. We have previously utilized a variety of other *in vitro*-based approaches to study this question, such as the gel mobility shift assay and gel filtration chromatography (Cheskis & Freedman, 1994). While these techniques provided us with very important structural and functional insights about how ligands can modulate the dimerization states of these receptors, only kinetic analyses could explain at what level such interactions were being influenced.

Using surface plasmon resonance, we have found that 1,25-$(OH)_2D_3$ binding significantly reduces the affinity of VDR homodimerization, decreasing the association rate of VDR−VDR interaction and increasing the off-rate. It is likely that ligand-induced conformational changes in the receptor (Allan *et al*., 1992; Keidel *et al*., 1994) make VDR homodimerization more difficult. At the same time, binding of 1,25-$(OH)_2D_3$ by VDR enhances the affinity of VDR−RXR heterodimerization. The kinetic data here indicate that the enhancement of heterodimerization by the ligand occurs primarily at the level of the rate of association (Table 1). In doing so, 1,25-$(OH)_2D_3$ increases the concentration of VDR−RXR heterodimers in solution, which then significantly enhances VDR−RXR complex formation on DNA. In the presence of 9-*cis*-retinoic acid, the concentration of the heterodimer is lower relative to when the ligand is absent; in addition, the rate of heterodimer association with DNA is lower when RXR is liganded. Thus, 9-*cis*-RA significantly reduces the overall affinity of the VDR−RXR heterodimeric complex. Simultaneously, 9-*cis*-RA increases RXR homodimerization, leaving less RXR available to complex with VDR. The combined effect in vivo would be a decrease in the concentration of VDR−RXR heterodimers able to bind to DNA and trans-activate from VDRE elements; in several transient transfection experiments, such an attenuating effect by 9-*cis*-RA has been observed (MacDonald *et al*., 1993; Freedman *et al*., 1994b; Lemon & Freedman, 1996).

Figure 9 illustrates how 1,25-$(OH)_2D_3$ binding modulates the free energy change of VDR interaction with itself, RXR and DNA. It is apparent that ligand binding results in strong positive cooperativity that drives VDR−RXR heterodimerization and as a result DNA binding. On the other hand, 1,25-$(OH)_2D_3$ binding results in a negative cooperativity imposed on VDR−VDR or VDR−DNA interaction. It is striking that the same ligand can drive the equilbrium so strongly for the heterodimer, while actively disrupting the homodimer. There is also negative cooperativity by 9-*cis*-RA binding on VDR−RXR interaction with DNA.

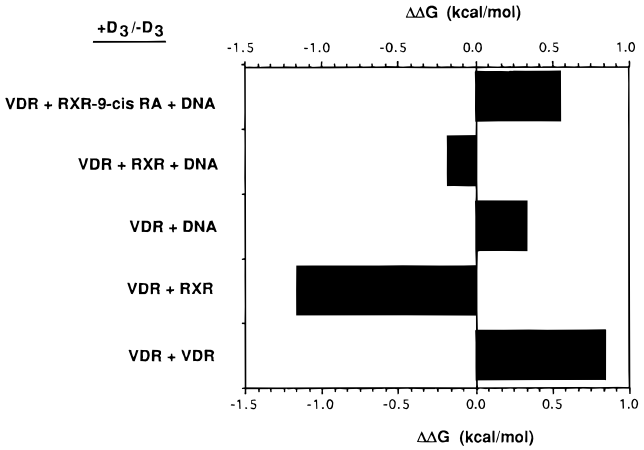

FIGURE 9: Effect of 1,25-$(OH)_2D_3$ binding on the change of free energy of VDR interactions with RXR and/or DNA. Free energies of protein−protein and protein−DNA interaction were calculated from the equilibrium dissociation constants ($\Delta\Delta G = -RT \ln K_1/K_2$, where K_1 and K_2 are equilibrium dissociation constants for the unliganded and liganded complex).

In this work, we have shown that at least one role of nuclear receptor ligands is to regulate receptor dimerization both in solution and on DNA. The ligands appear to do so dynamically, modulating the overall affinity of these complexes. This mechanism therefore creates a fast and sensitive way to regulate DNA binding in response to changes in ligand concentration. Since there is a direct correlation between the effects of these and other ligands on formation of receptor−DNA complexes *in vitro* and transcriptional activation *in vivo* (Cheskis & Freedman, 1994; Lehmann *et al.*, 1993; Miyamoto *et al.*, 1993; Yen *et al.*, 1992; Zhang *et al.*, 1992; MacDonald *et al.*, 1993; Freedman *et al.*, 1994b; Lemon & Freedman, 1996), we believe that this kind of detailed kinetic study may add to our understanding of how transcription may be regulated by this family of proteins. It will be of interest to test how structural changes in vitamin D and retinoids may affect the kinetics of VDR and RXR interactions. Conceivably, a growing number of potentially clinically important synthetic hormonal analogues may act by subtly but decisively altering the activity of these receptors at the level of dimerization in a manner distinct from the natural ligands. Work is currently underway in our laboratory using SPR to test this hypothesis (Cheskis & Freedman, 1995).

ACKNOWLEDGMENT

We are indebted to Peter Lomedico of Morphogenesis, Inc., and Russ Granzow of Pharmacia Biosensor for their ongoing help during this project and to Milan Uskokovec for supplying 1,25-dihydroxyvitamin D_3. We thank Ben Luisi and Marilyn Resh for their comments and suggestions.

REFERENCES

Allan, G. F., Leng, X., Tsai, S. Y., Weigel, N. L., Edwards, D. P., Tsai, M.-J., & O'Malley, B. W. (1992) *J. Biol. Chem. 267,* 19513−19520.

Amero, S. A., Kretsinger, R. H., Moncrief, N. D., Yamamoto, K. R., & Pearson, W. R. (1992) *Mol. Endocrinol. 6,* 3−7.

Andersson, M. L., Nordstrom, K., Demczuk, S., Harbers, M., & Vennstrom, B. (1992) *Nucleic Acids Res. 20,* 4803−10.

Bondeson, S., Frostell-Karlsson, Å., Fägerstam, L., & Magnusson, G. (1993) *Anal. Biochem. 214,* 245−251.

Cheskis, B., & Freedman, L. P. (1994) *Mol. Cell. Biol. 14,* 3329−3338.

Cheskis, B., & Freedman, L. P. (1995) *Mol. Endocrinol. 9,* 1814−1824.

Fisher, R. J., Fivash, M., Casas-Finet, J., Erickson, J. W., Kondoh, A., Bladen, S. V., Fisher, C., Watson, D. K., & Papas, T. (1994a) *Protein Sci. 3,* 257−266.

Fisher, R. J., Fivash, M., Casas-Finet, M., Bladen, S., & Marson McNitt, K. (1994b) *Methods: Companion Guide Methods Enzymol. 6,* 121−133.

Freedman, L. P., Arce, V., & Perez Fernandez, R. (1994a) *Mol. Endocrin. 8,* 265−273.

Freedman, L. P., Cheskis, B., Lemon, B. D., Liu, M., & Towers, T. L. (1994b) In *Vitamin D, A Pluripotent Steroid Hormone: Structural Studies, Molecular Endcrinology, and Clinical Applications* (Norman, A., Bouillon, R., & Thomasset, M., Ed.) pp 217−225, Walter de Gruter, New York.

Granzow, R., & Reed, R. (1992) *BioTechnology 10,* 390−393.

Karlsson, R. Michaelsson, A., & Mattsson, L. (1991) *J. Immunol. Methods 145,* 229−240.

Keidel, S., LeMotte, P., & Apfel, C. (1994) *Mol. Cell. Biol. 14,* 287−298.

Laudet, V., Hanni, C., Coll, J., Catzeflis, F., & Stehlin, D. (1992) *EMBO J. 11,* 1003−1013.

Lehmann, J. M., Zhang, X.-K., Graupner, G., Lee, M.-O., Hermann, T., Hoffmann, B., & Pfahl, M. (1993) *Mol. Cell. Biol. 13,* 7698−7707.

Lemon, B. D., & Freedman, L. P. (1996) *Mol. Cell. Biol.* (in press).

Löfas S., & Johnson B. (1990) *J. Chem. Soc., Chem. Commun. 21,* 1526−1528.

MacDonald, P. N., Dowd, D. R., Nakajama, S., Galligan, M. A., Reeder, M. C., Haussler, C. A., Ozato, K., & Haussler, M. R. (1993) *Mol. Cell. Biol. 13,* 5907−5917.

Mangelsdorf, D. J., Umesono, K., Kliewer, S. A., Borgmeyer, U., Ong, E. S., & Evans, R. M. (1991) *Cell 66,* 555−561.

Miyamoto, T., Suzuki, S., & DeGroot, L. J. (1993) *Mol. Endocrinol. 7,* 224−231.

Nishikawa, J., Kitaura, M., Imagawa, M., & Nishihara, T. (1995) *Nucleic Acids Res. 23,* 606−611.

Noda, M., Vogel, R. L., Craig, A. M., Prahl, J., DeLuca, H. F., & Denhardt, D. T. (1990) *Proc. Natl. Acad. Sci. U.S.A. 90,* 9995−9999.

Towers, T. L., Luisi, B. L., Asianov, A., & Freedman, L. P. (1993) *Proc. Natl. Acad. Sci. U.S.A. 90,* 6310−6314.

Yen, P. M., Sugawara, A., & Chin, W. W. (1992) *J. Biol. Chem. 267,* 23248−23252.

Zhang, X. K., Lehmann, J., Hoffmann, B., Dawson, M. I., Cameron, J., Graupner, G., Hermann, T., Tran, P., & Pfahl, M. (1992) *Nature 358,* 587−591.

BI952283R